# Magnetic and Mössbauer Spectroscopic Characterization of $EuNi_2Sb_2$

Inga Schellenberg, Matthias Eul, and Rainer Pöttgen

Institut für Anorganische und Analytische Chemie,
Westfälische Wilhelms-Universität Münster,
Corrensstraße 30, 48149 Münster, Germany

Reprint requests to R. Pöttgen.
E-mail: pottgen@uni-muenster.de

*Z. Naturforsch.* **2011**, *66b,* 1179 – 1182;
received October 24, 2011

$ThCr_2Si_2$-type $EuNi_2Sb_2$ ($I4/mmm$, $a$ = 438.1(1), $c$ = 1068.1(4) pm) was synthesized by arc-melting of the elements. Magnetic susceptibility measurements show Curie-Weiss behavior with an experimental magnetic moment of 8.03(1) $\mu_B$/Eu atom, indicating stable divalent europium. $EuNi_2Sb_2$ orders antiferromagnetically at $T_N$ = 5.8(1) K. A $^{151}$Eu Mössbauer spectrum at 4.2 K shows two spectral components with hyperfine fields of 19.1 and 12.9 T, indicative of different magnetically ordered domains.

*Key words:* Europium, Antimonide,
Mössbauer Spectroscopy

## Introduction

The antimonides $EuT_2Sb_2$ ($T$ = Mg, Mn, Ni, Cu, Zn, Pd, Cd, Pt) [1 and refs. cited therein] crystallize with simple structures that derive from the $ThCr_2Si_2$, $CaBe_2Ge_2$ or $CaAl_2Si_2$ type. The europium atoms show magnetic ordering at low temperatures, and a maximum Néel temperature of 13.3 K was observed for $EuZn_2Sb_2$ [2]. Only the transition metal substructure of $EuMn_2Sb_2$ [3] orders magnetically at around 600 K.

$EuNi_2Sb_2$ has first been reported by Marchand and Jeitschko [4], and the structure was refined on the basis of single-crystal diffractometer data [5]. However, so far no physical properties have been determined. In the course of our systematic studies on $ThCr_2Si_2$- and $CaBe_2Ge_2$-related compounds [1, 3, 6, and refs. therein] we have determined the magnetic and Mössbauer spectroscopic behavior of this antimonide.

## Experimental Section

### *Synthesis*

Starting materials for the preparation of the $EuNi_2Sb_2$ sample were ingots of sublimed europium (Johnson Matthey), nickel wire (Johnson Matthey) and antimony shots (ABCR), all with stated purities better than 99.9 %. The air- and moisture-sensitive europium pieces were kept under argon prior to the reaction. The argon was purified before with titanium sponge (870 K), silica gel and molecular sieves. Europium, nickel, and antimony were weighed in the ideal 1 : 2 : 2 atomic ratio and reacted by arc-melting under argon [7]. The product pellet was remelted three times in order to ensure homogeneity. The total weight loss after the melting procedures was less than 0.5 %. The $EuNi_2Sb_2$ sample is silvery with metallic luster and stable in air over months.

### *Powder X-ray diffraction*

The polycrystalline $EuNi_2Sb_2$ sample was characterized by powder X-ray diffraction: Guinier camera, Cu$K_{\alpha1}$ radiation, $\alpha$-quartz ($a$ = 491.30, $c$ = 540.46 pm) as internal standard, and an imaging plate technique (Fujifilm, BAS-READER 1800). The tetragonal lattice parameters ($a$ = 438.1(1), $c$ = 1068.1(4) pm) were deduced from a least-squares refinement. The experimental pattern was compared to a calculated one [8] to ensure correct indexing. Our data compare well with the ones reported by Marchand and Jeitschko ($a$ = 438.34(6), $c$ = 1066.4(1) pm) [4].

### *Susceptibility measurements*

Magnetic susceptibility measurements were carried out on a Quantum Design Physical Property Measurement System (PPMS) using the VSM option. For the measurements, 7.574 mg of the $EuNi_2Sb_2$ sample were packed in kapton foil and attached to the sample holder rod for measuring the magnetic properties in the temperature range 2.5 – 300 K with magnetic flux densities up to 80 kOe.

### *Mössbauer spectroscopy*

The 21.53 keV transition of $^{151}$Eu with an activity of 130 MBq (2 % of the total activity of a $^{151}Sm:EuF_3$ source) and a $Ba^{121m}SnO_3$ source were used for the Mössbauer spectroscopic characterization. The measurements were conducted in transmission geometry with a commercial helium-bath cryostat. The temperature of the absorber was varied between 4.2 K and r. t., while the source was kept at r. t. The temperature was controlled by a resistance thermometer (±0.5 K accuracy). The sample thickness (PVC container) corresponds to about 10 mg of the Mössbauer-active element/cm$^2$.

## Results and Discussion

### *Crystal chemistry*

$EuNi_2Sb_2$ adopts the tetragonal $ThCr_2Si_2$-type structure, space group $I4/mmm$. The nickel atoms

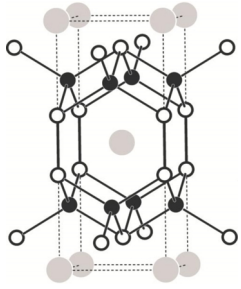

Fig. 1. View of the $EuNi_2Sb_2$ structure approximately along the *y* axis. Europium, nickel and antimony atoms are drawn as medium grey, black filled and open circles, respectively. The three-dimensional $[Ni_2Sb_2]$ network is emphasized.

have tetrahedral antimony coordination (Fig. 1). A view on the crystal structure approximately along the *y* axis is presented in Fig. 1. The $NiSb_4$ tetrahedra are condensed *via* common edges to layers and *via* Sb–Sb bonds (299 pm [5]) to a three-dimensional network in which the divalent europium atoms (*vide infra*) fill the large cavities. The crystal chemistry of $ThCr_2Si_2$-related structures has repeatedly been discussed. For further details and literature overviews we refer to [6, 9, and refs. therein].

As was evident from single-crystal data [5], $EuNi_2Sb_2$ adopts a small homogeneity range $EuNi_{2-x}Sb_2$. A structure refinement revealed a composition $EuNi_{1.53}Sb_2$ and lattice parameters $a$ = 434.0(1), $c$ = 1059.7(5) pm, smaller than those originally reported for $EuNi_2Sb_2$ [4]. Since our lattice parameters (*vide supra*) are close to the data reported in [4], we conclude that the composition of our sample is close to the ideal one.

*Magnetic properties*

The $\chi(T)$ and $\chi^{-1}(T)$ data of $EuNi_2Sb_2$ measured at 10 kOe are shown in Fig. 2. In the temperature range of 25 – 300 K the data could be fitted with the Curie-Weiss law, revealing an effective magnetic moment of $\mu_{eff}$ = 8.03(1) $\mu_B$/Eu atom and a Weiss constant of $\theta_P$ = −8.5 K. The effective magnetic moment is in good agreement with the theoretical value for $Eu^{2+}$ of 7.94 $\mu_B$ and thus also confirms the composition $EuNi_2Sb_2$. If one would assume the nickel-deficient phase $EuNi_{1.53}Sb_2$ one obtains a reduced moment of only 7.79 $\mu_B$/Eu atom. The negative $\theta_P$ is indicative of antiferromagnetic interactions. At around 5 K antiferromagnetic ordering is evident from the $\chi(T)$ data. To determine the exact Néel temperature ($T_N$),

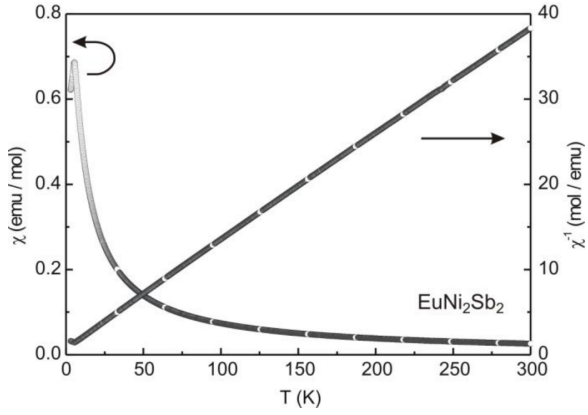


Fig. 2. Temperature dependence of the magnetic susceptibility ($\chi$ and $\chi^{-1}$ data) of $EuNi_2Sb_2$ measured at 10 kOe.

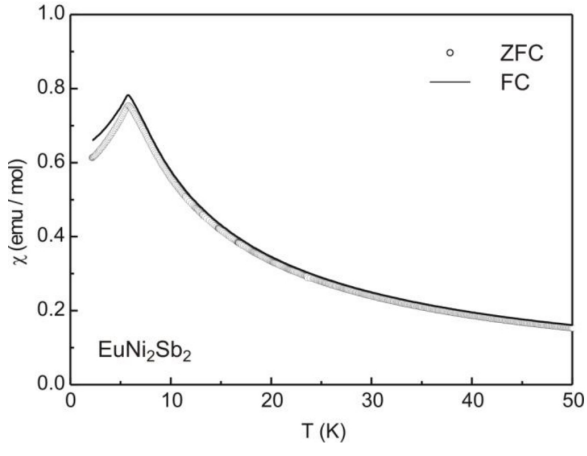


Fig. 3. Susceptibility measurements at 100 Oe of $EuNi_2Sb_2$ in the zero field-cooled (ZFC) and field-cooled (FC) mode.

low-field susceptibility measurements were performed. The susceptibility in an external field of 100 Oe was first measured in a zero field-cooled and additionally in a field-cooled state in the temperature range of 2.5 – 50 K (Fig. 3). An antiferromagnetic transition at 5.8(1) K was observed. Fig. 4 displays the magnetization isotherms taken at different temperatures. The magnetization isotherm above the ordering temperature at 50 K shows a linear increase of magnetization with the application of an external field, as is expected for a paramagnetic material. Close to the ordering temperature, the isotherm at 10 K reveals a slight curvature at high fields. Below the ordering temperature at 3 K the magnetization isotherm displays a metamagnetic step starting at around 20 kOe. The magnetization isotherm at 3 K shows a saturation magnetization of

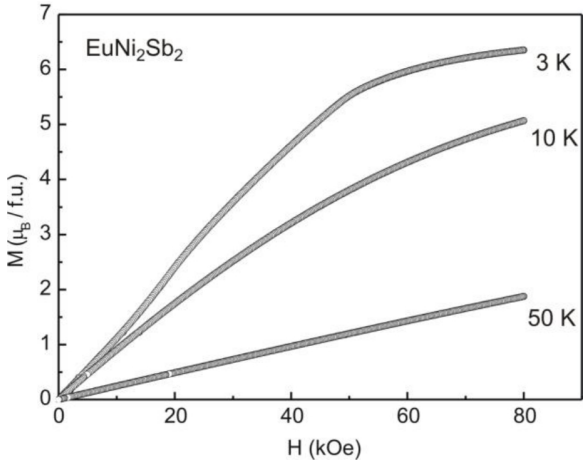


Fig. 4. Magnetization isotherms of $EuNi_2Sb_2$ measured at 3 (below $T_N$), 10 and 100 K.

approximately 6.4 $\mu_B$/Eu atom at 80 kOe, close to the maximum theoretical value of $g_J \times S = 7\ \mu_B/Eu^{2+}$. The $M(H)$ behavior below the ordering temperature is non-hysteretic, and together with the observed metamagnetic behavior manifests the antiferromagnetic ground state.

### *$^{121}$Sb and $^{151}$Eu Mössbauer spectroscopic characterization*

The $^{151}$Eu Mössbauer spectra of the $EuNi_2Sb_2$ sample at 298, 77, and 4.2 K are presented in Fig. 5 together with transmission integral fits. The corresponding fitting parameters are summarized in Table 1. At 298 and 77 K, well above the magnetic ordering temperature, the spectra could be fitted with a single signal at an isomer shift close to 11.3 mm s$^{-1}$, indicative of purely divalent europium, in agreement with the susceptibility measurements. The experimental line width is slightly increased with respect to the typical value of around 2.3 mm s$^{-1}$ observed for intermetallic compounds. This may indicate small inhomogeneities in the sample (*vide infra*).

At 4.2 K, in the magnetically ordered regime, magnetic hyperfine field splitting was observed. However, the spectrum could only be well reproduced by a superposition of two spectral components. The main component with 60 % contribution at $\delta = -11.41(4)$ mm s$^{-1}$ shows a magnetic hyperfine field of 19.1(1) T, typically observed for europium intermetallics [10]. This signal is superimposed by a second contribution of 40 % at $\delta = -11.23(6)$ mm s$^{-1}$ and a smaller hyperfine field of only 12.9(2) T. This behavior can only be explained by a domain structure within the sample. The major part of the sample shows full magnetic ordering, while in the other domains long-range magnetic ordering is still

Table 1. Fitting parameters of $^{121}$Sb and $^{151}$Eu Mössbauer spectroscopic measurements of $EuNi_2Sb_2$. Numbers in parentheses represent the statistical errors in the last digit. ($\delta$), isomer shift; ($\Gamma$), experimental line width; ($\Delta E_Q$), electric quadrupole splitting; ($B_h$), magnetic hyperfine field. Numbers marked with an asterisk were fixed during the fitting procedure.

| Source | $T$ (K) | $\delta$ (mm s$^{-1}$) | $\Gamma$ (mm s$^{-1}$) | $\Delta E_Q$ (mm s$^{-1}$) | $B_h$ (T) | ratio (%) |
|---|---|---|---|---|---|---|
| $^{121}$Sb | 77 | −8.27(7) | 3.4(3) | −0.25(3) | – | – |
| $^{151}$Eu | 298 | −11.32(3) | 3.36(8) | 0.0* | – | – |
| | 77 | −11.19(2) | 2.49(9) | −2.70(3) | – | – |
| | 4.2 | −11.41(4) | 2.6* | 3.5(2) | 19.1(1) | 60 |
| | 4.2 | −11.23(6) | 2.6* | −1.9(4) | 12.9(2) | 40 |

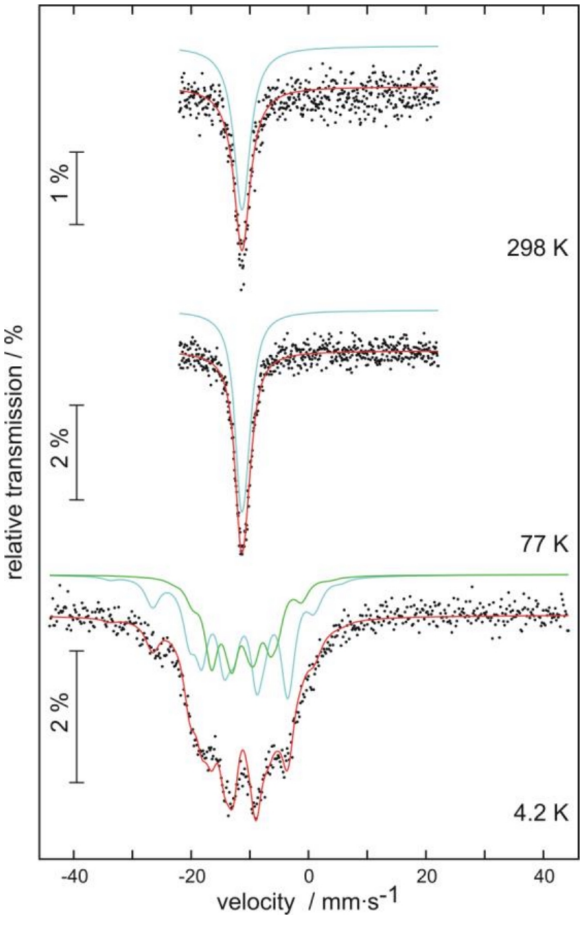


Fig. 5 (color online). Experimental and simulated $^{151}$Eu Mössbauer spectra of $EuNi_2Sb_2$ at 298, 77 and 4.2 K.

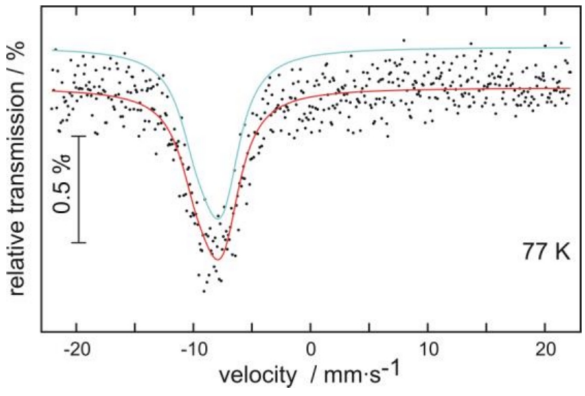


Fig. 6 (color online). Experimental and simulated $^{121}$Sb Mössbauer spectrum of $EuNi_2Sb_2$ at 77 K.

not complete at 4.2 K. This spectroscopic result indicates small inhomogeneities within the $EuNi_2Sb_2$ sample, most likely domains of $EuNi_{2-x}Sb_2$ with a very small value of $x$. Such domains are most likely also the reason for the slightly enhanced line width observed at r. t.

The $^{121}$Sb spectrum (Fig. 6) could be well reproduced with a single antimony site. In the fit only a moderate quadrupole splitting of around $-0.25\ \mathrm{mm\,s^{-1}}$ occurs. The $^{121}$Sb isomer shift compares very well with the ones determined for other intermetallic antimony compounds such as $RET_2Sb_2$ ($RE$ = Eu, Yb; $T$ = Zn, Mn, Pd) [1, 3] or Yb$T$Sb ($T$ = Ni, Pd, Pt, Cu, Ag, Au) [11]. Moreover, it is in line with those given in an overview of different antimony compounds by Lippens [12].

*Acknowledgement*

This work was financially supported by the Deutsche Forschungsgemeinschaft.

[1] I. Schellenberg, M. Eul, R. Pöttgen, *Z. Naturforsch.* **2010**, *65b*, 18.
[2] F. Weber, A. Cosceev, A. Nateprov, C. Pfleiderer, A. Faißt, M. Uhlarz, H. von Löhneysen, *Physica B* **2005**, *359 – 361*, 226.
[3] I. Schellenberg, M. Eul, W. Hermes, R. Pöttgen, *Z. Anorg. Allg. Chem.* **2010**, *636*, 85.
[4] R. Marchand, W. Jeitschko, *J. Solid State Chem.* **1978**, *24*, 351.
[5] W. K. Hofmann, W. Jeitschko, *J. Less-Common Met.* **1988**, *138*, 313.
[6] D. Kußmann, R. Pöttgen, U. Ch. Rodewald, C. Rosenhahn, B. D. Mosel, G. Kotzyba, B. Künnen, *Z. Naturforsch.* **1999**, *54b*, 1155.
[7] R. Pöttgen, Th. Gulden, A. Simon, *GIT Labor-Fachzeitschrift* **1999**, *43*, 133.
[8] K. Yvon, W. Jeitschko, E. Parthé, *J. Appl. Crystallogr.* **1977**, *10*, 73.
[9] E. Parthé, L. Gelato, B. Chabot, M. Penzo, K. Cenzual, R. Gladyshevskii, TYPIX – Standardized Data and Crystal Chemical Characterization of Inorganic Structure Types, *Gmelin Handbook of Inorganic and Organometallic Chemistry*, 8th ed., Springer, Berlin, **1993**.
[10] R. Pöttgen, D. Johrendt, *Chem. Mater.* **2000**, *12*, 875.
[11] R. Mishra, R. Pöttgen, R. -D. Hoffmann, Th. Fickenscher, M. Eschen, H. Trill, B. D. Mosel, *Z. Naturforsch.* **2002**, *57b*, 1215.
[12] P. E. Lippens, *Solid State Commun.* **2000**, *113*, 399.